

Large-Scale Numerical-Diagonalization Study of the Shastry-Sutherland Model

Hiroki NAKANO¹ and Tôru SAKAI^{1,2}

¹*Graduate School of Science, University of Hyogo, Kamigori, Hyogo 678-1297, Japan*

²*National Institutes for Quantum and Radiological Science and Technology, SPring-8 Sayo, Hyogo 679-5148, Japan*

E-mail: hnakano@sci.u-hyogo.ac.jp

(Received July 14, 2022)

The $S = 1/2$ Heisenberg antiferromagnet on the orthogonal-dimer lattice (Shastry-Sutherland model) is studied by the Lanczos diagonalization method. The properties of this model are determined by the ratio of two interactions, namely, $r = J_2/J_1$, where J_1 denotes the amplitude of spin interactions at orthogonal dimers and the interactions represented by J_2 form the square lattice. We focus our attention on the edge of the phase in which the dimer state is realized as the exact ground state. Our large-scale calculations of diagonalizations treating finite-size clusters including 44 and 48 spin sites successfully detect the target edge. Our conclusion is that the ratio for the edge is $r = 0.6754(2)$. This estimate is compared with an experimental result from electron spin resonance measurements.

KEYWORDS: $S = 1/2$ Heisenberg antiferromagnet, orthogonal-dimer lattice, Lanczos diagonalization, parallel calculations

1. Introduction

The Shastry-Sutherland model – the $S = 1/2$ Heisenberg antiferromagnet on the orthogonal-dimer lattice – has attracted considerable attention as a typical frustrated magnet [1]. The most characteristic behavior of this model is that the system realizes the ground state that can be expressed by the mathematically exact quantum state, namely, the singlet-dimer state, when the ratio J_2/J_1 is smaller than a specific value, where J_1 and J_2 denote the orthogonal-dimer interaction and the interaction forming the square lattice, respectively. On the other hand, the Néel-ordered ground state is realized when the ratio J_2/J_1 is sufficiently large. However, the properties of this model are still unclear in and near the intermediate range between the exact dimer state and the Néel-ordered state. $\text{SrCu}_2(\text{BO}_3)_2$ is a good candidate material for this model [2]; it is considered that this material corresponds to the case when the ratio J_2/J_1 is in the exact dimer phase. Recent experimental reports have shown that the ratio can be changed under pressure and that one can detect the edge of the exact dimer phase [3, 4]. On the other hand, it is still difficult to precisely determine the phase transition points theoretically during the variation of J_2/J_1 because of the strong frustration in this model. In several numerical studies, the estimation of the transition points has been tackled. Among numerical-diagonalization studies, the Shastry-Sutherland model has been investigated for finite-size clusters with sizes up to 40 spin sites [5].

Let us focus our attention on the phase boundary between the exact dimer phase and its neighboring phase. This boundary has been experimentally detected as mentioned before. If we obtain a theoretical result for the boundary as a precise estimate, the experimental and theoretical results can be compared; it will contribute much to our understanding of this system. Under such circumstances, the purpose of this study is to estimate the ratio J_2/J_1 for this boundary from additional results of system sizes that have not been treated before. In this study, we successfully carried out Lanczos

diagonalization calculations to obtain the ground-state energy of finite-size clusters larger than those in previous studies. Our calculations enable us to obtain a highly precise estimation for the transition point for the edge of the exact dimer phase. Our additional results show a weak system-size dependence of the ratio for the transition point. Our estimation for the transition point will be compared with an experimental observation.

This paper is organized as follows. In the next section, we will introduce the model Hamiltonian and explain our numerical method. In the third section, we will present and discuss our results. In the final section, we will summarize the results of this study and provide some remarks.

2. Hamiltonian and Method

The Hamiltonian studied here is given by

$$\mathcal{H} = \sum_{\langle i,j \rangle: \text{orthogonal dimer}} J_1 \mathbf{S}_i \cdot \mathbf{S}_j + \sum_{\langle i,j \rangle: \text{square lattice}} J_2 \mathbf{S}_i \cdot \mathbf{S}_j, \quad (1)$$

where \mathbf{S}_i denotes the $S = 1/2$ spin operator at site i . Here, we consider the case of an isotropic interaction in spin space. Site i is assumed to characterize the vertex of the square lattice. The number of spin sites is represented by N_s . The first and second terms of Eq. (1) denote orthogonal dimer interactions represented by thick solid bonds in Fig. 1 and interactions forming the square lattice represented by thin solid bonds in Fig. 1, respectively. The two interactions between the two spins are antiferromagnetic, namely, $J_1 > 0$ and $J_2 > 0$. Note here that energies are measured in units of J_1 ; hereafter, we set $J_1 = 1$. The ratio J_2/J_1 is denoted by r ; when $r = 0$, the system is an assembly of isolated dimerized-spin models; on the other hand, the system in the limit $r \rightarrow \infty$ is reduced to the $S = 1/2$ Heisenberg antiferromagnet on the ordinary square lattice. We treat finite-size clusters with system size N_s under the periodic boundary condition. In this study, we additionally treat $N_s = 44$ and 48; finite-size clusters for these cases are shown in Fig. 1. Unfortunately, finite-size clusters for $N_s = 44$ and 48 cannot form squares even if the squares are tilted; therefore, the treated clusters are not squares. Even under this situation, calculations for the treated clusters can provide us with significant information concerning this system.

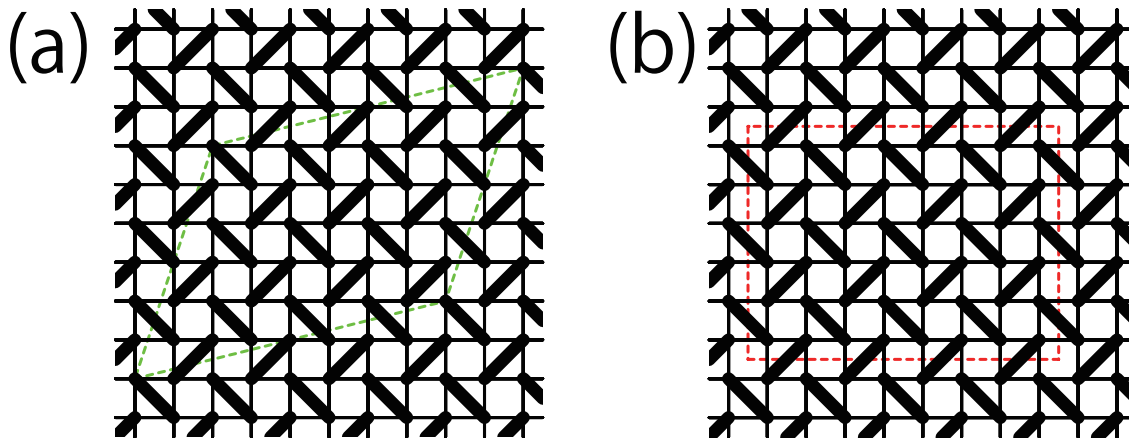


Fig. 1. Structure of the orthogonal-dimer lattice and its finite-size clusters. Thick and thin solid lines denote bonds for J_1 and J_2 , respectively. Panel (a) shows the finite-size cluster of $N_s = 44$ indicated by green dotted lines. Panel (b) shows the finite-size cluster of $N_s = 48$ indicated by red dotted lines.

In this study, numerical diagonalizations are carried out on the basis of the Lanczos algorithm to

obtain the lowest energy of \mathcal{H} in the subspace characterized by $\sum_j S_j^z = M$. The z -axis is taken as the quantized axis of each spin. Numerical-diagonalization calculations are widely considered to be unbiased. Thus, one can obtain reliable information about the target system. The energy is represented by $E(N_s, M)$; here, we calculate the energy in the case of $M = 0$ because our attention is focused primarily on the behavior of the ground-state energy $E_g = E(N_s, 0)$. Some of the Lanczos diagonalizations were carried out using the MPI-parallelized code that was originally developed in the study of Haldane gaps [6]. The usefulness of our program was confirmed in large-scale parallelized calculations in various studies [5, 7–9]. Our largest-scale calculations for $N_s = 48$ in this study have been carried out using Fugaku. The calculations for $N_s = 48$ in Fugaku use 65536 nodes that correspond to approximately 41% of the nodes in Fugaku. Note here that the dimension of $N_s = 48$ and $M = 0$ is 32,247,603,683,100 and that this dimension is larger than 18,252,025,766,941 in the case of $N = 30$ for $S = 1$ in which Lanczos diagonalization was successfully carried out in Ref. 9.

3. Results and Discussion

In this study, the ratio of interactions for the edge of the exact dimer phase is focused on; this ratio is denoted by r_{c1} hereafter. Before presenting our results, let us review previous estimates of r_{c1} . Estimates of r_{c1} are summarized in chronological order in Table I. Note here that Refs. 5, 11, and 15 were based on the method of numerical diagonalizations. On the other hand, in Refs. 16 and 17, a type of calculation based on a tensor-network framework was employed. In Ref. 14, a series expansion method was used. Note that Ref. 14 was the first report that pointed out the existence of an intermediate phase between the exact dimer and Néel-ordered phases.

Table I. Estimates of the ratio of interactions r_{c1} corresponding to the edge of the exact dimer phase from various theoretical approaches.

Ref.	Publication year	r_{c1}	Method
10	1996	0.6	Schwinger boson mean field theory
11	1999	0.70(1)	Numerical Diagonalization (up to 20 sites)
12	1999	0.691(6)	Ising Expansion
13	2000	0.697(2)	Dimer Expansion
14	2000	0.677(2)	Plaquette Expansion
15	2002	0.678	Numerical Diagonalization (up to 32 sites)
16	2012	0.687(3)	Tensor Network with MERA
17	2013	0.675(2)	Tensor Network with iPEPS
5	2018	0.675	Numerical Diagonalization (36 and 40 sites)
This study	present	0.6754(2)	Numerical Diagonalization (44 and 48 sites)

Now, let us observe the r -dependence of the ground state energy of the Hamiltonian (1); the results are shown in Fig. 2. One finds that our calculations for both $N_s = 44$ and 48 have succeeded in capturing the energy level ($E_g = -(3/8)N_s$) of the exact dimer state in the region of small r . In Fig. 2, this energy level is shown by the broken line for each N_s . In the region where r becomes larger than a specific value, the ground state energy at the same time becomes lower than the energy level of the exact dimer state. In Fig. 2, we draw a fitting line determined from the two data points that are close to the energy level of the exact dimer state. Let us focus our attention on large- r data points that are distant from the energy level of the exact dimer state. One also confirms that these points fall on the fitting line, although these points are not used for the fitting. This behavior suggests that in the range of large r in Fig. 2, there appears a spin state that differs from the exact dimer state. From the point where the horizontal broken line and the solid fitting line cross, we can obtain the information

concerning the edge of the exact dimer phase. Therefore, our present results are

$$r_{c1} = 0.67551, \quad (2)$$

for $N_s = 44$ and

$$r_{c1} = 0.67542, \quad (3)$$

for $N_s = 48$. One can recognize that the difference between Eqs. (2) and (3) is quite small.

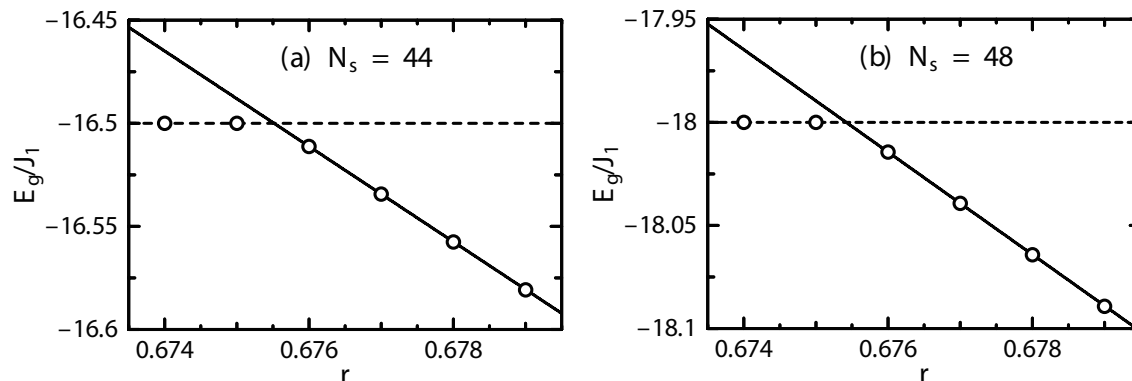


Fig. 2. Ground state energy for $N_s = 44$ and 48 in panels (a) and (b), respectively. Circles denote numerical-diagonalization results. Horizontal broken lines represent the energy level of the exact dimer state. Solid lines are obtained by the fitting based on the two points that are close to the energy level of the exact dimer state.

Next, let us examine the results of Eqs. (2) and (3) together with those reported previously in the studies based on the numerical-diagonalization method. The comparison is shown in Fig. 3. When N_s decreases, r_{c1} shows a significantly large system-size dependence up to $N_s = 32$. On the other hand, the differences in estimated r_{c1} between neighboring data points become much smaller for N_s larger than 40. This behavior strongly suggests that our additional results for $N_s = 44$ and 48 include only small finite-size deviations from the value in the thermodynamic limit. If the investigations treating even larger N_s based on the diagonalization method were carried out, it would be expected that differences between neighboring data points for r_{c1} become smaller. It is presently reasonable that an error is determined so that there are Eqs. (2) and (3) within the error. Consequently, the final conclusion of this study is

$$r_{c1}^{(th)} = 0.6754(2). \quad (4)$$

Let us discuss Eq. (4) from the viewpoint of the comparison with the estimate in an experimental report. In Ref. 4, Sakurai *et al.* carried out electron spin resonance measurements under high pressure and high field. They finally reported

$$r_{c1}^{(ex)} = 0.660 \pm 0.003. \quad (5)$$

Then, one finds the difference to be

$$\left| r_{c1}^{(ex)} - r_{c1}^{(th)} \right| \sim 0.015. \quad (6)$$

The difference strongly suggests that the presence of other effects should be taken into account in addition to the simple Shastry-Sutherland Hamiltonian (1). A high possibility is the presence of

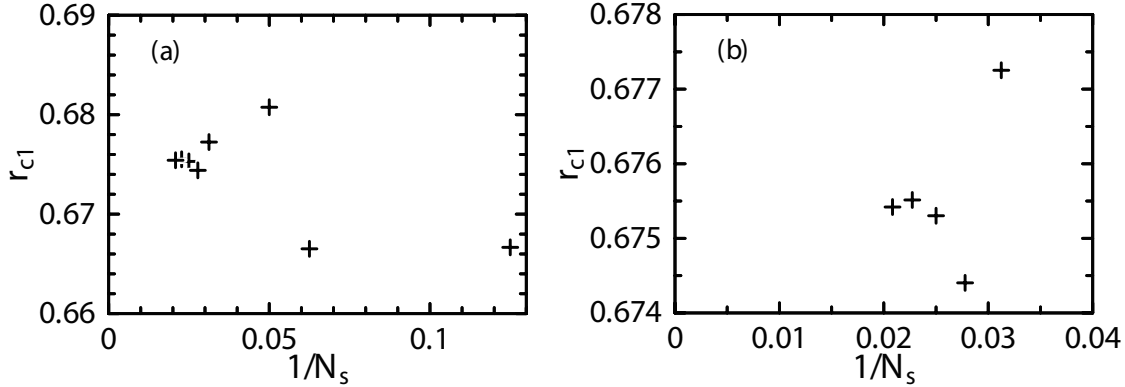


Fig. 3. System-size dependence of the ratio for the edge of the exact dimer phase. Panel (a) shows the entire range from $N_s = 8$ to 48. Panel (b) is a magnified view in the range from $N_s = 32$ to 48.

Dzyaloshinski-Moriya interactions. In Ref. 4, Sakurai *et al.* also reported $J_1 = 69.1$ K, $J_2/J_1 = 0.601$, and $D = 1.6$ K at ambient pressure, where D denotes the amplitude of the Dzyaloshinski-Moriya interaction along the c -axis on the bond forming the square lattice, namely, the bond of J_2 ; therefore, the ratio of their estimates is found to be $D/J_1 \sim 0.023$. The relationship between this ratio and Eq. (6) should be examined in future studies together with other possibilities.

4. Summary and Remarks

We have studied the $S = 1/2$ Heisenberg antiferromagnet on the orthogonal-dimer lattice by the Lanczos diagonalization method. The boundary between the exact dimer phase and the neighboring phase is focused on; the corresponding ratio J_2/J_1 is found to be 0.6754(2). Future studies should tackle estimations for other phase boundaries. One of them is the boundary between the Néel-ordered phase and an intermediate phase. Various estimates for this boundary in previous studies showed deviations that are more serious than the finite-size deviations of r_{c1} . The other is the boundary inside the intermediate region reported in Ref. 5. Such studies will greatly contribute to our fundamental understanding of magnetic materials with frustration.

Acknowledgments

This work was partly supported by JSPS KAKENHI Grant Numbers 16K05419, 16H01080(J-Physics), 18H04330(J-Physics), JP20K03866, and JP20H05274. In this research, we used the computational resources of the supercomputer Fugaku provided by RIKEN through the HPCI System Research projects (Project IDs: hp200173, hp210068, hp210127, hp210201, and hp220043). Some of the computations were performed using facilities of the Institute for Solid State Physics, The University of Tokyo.

References

- [1] B. S. Shastry and B. Sutherland, *Physica B+C* **108**, 1069 (1981).
- [2] H. Kageyama, K. Yoshimura, R. Stern, N. V. Mushnikov, K. Onizuka, M. Kato, K. Kosuge, C. P. Slichter, T. Goto, and Y. Ueda, *Phys. Rev. Lett.* **82**, 3168 (1999).
- [3] M. E. Zayed, Ch. Rüegg, J. Larrea J., A. M. Läuchli, C. Panagopoulos, S. S. Saxena, M. Ellerby, D. F. McMorrow, Th. Strässle, S. Klotz, G. Hamel, R. A. Sadykov, V. Pomjakushin, M. Boehm, M. Jiménez-Ruiz, A. Schneidewind, E. Pomjakushina, M. Stingaciu, K. Conder, and H. M. Rønnow, *Nat. Phys.*, **13**, 962 (2017).

- [4] T. Sakurai, Y. Hirao, K. Hijii, S. Okubo, H. Ohta, Y. Uwatoko, K. Kudo, and Y. Koike, *J. Phys. Soc. Jpn.* **87**, 033701 (2018).
- [5] H. Nakano and T. Sakai, *J. Phys. Soc. Jpn.* **87**, 123702 (2018).
- [6] H. Nakano and A. Terai, *J. Phys. Soc. Jpn.* **78**, 014003 (2009).
- [7] H. Nakano and T. Sakai, *J. Phys. Soc. Jpn.* **80**, 053704 (2011). [Errata **90**, 038002 (2021)]
- [8] H. Nakano, N. Todoroki, and T. Sakai, *J. Phys. Soc. Jpn.* **88**, 114702 (2019).
- [9] H. Nakano, H. Tadano, N. Todoroki, and T. Sakai, *J. Phys. Soc. Jpn.* **91**, 074701 (2022).
- [10] M. Albrecht and F. Mila, *Europhys. Lett.* **34**, 145 (1996).
- [11] S. Miyahara and K. Ueda, *Phys. Rev. Lett.* **82**, 3701 (1999).
- [12] Z. Weihong, C. J. Hamer, and J. Oitmaa, *Phys. Rev. B* **60**, 6608 (1999).
- [13] E. Muller-Hartmann and R. R. P. Singh, *Phys. Rev. Lett.* **84**, 1808 (2000).
- [14] A. Koga and N. Kawakami, *Phys. Rev. Lett.* **84**, 4461 (2000).
- [15] A. Läuchli, S. Wessel, and M. Sgrist, *Phys. Rev. B* **66**, 014401 (2002).
- [16] J. Lou, T. Suzuki, K. Harada, and N. Kawashima, arXiv:1212.1999.
- [17] P. Corboz and F. Mila, *Phys. Rev. B* **87**, 115144 (2013).